Corner Detection Using the MAP Technique

Xining Zhang, Robert M. Haralick, and Visvanathan Ramesh*
Department of EE, FT-10, University of Washington, Seattle, WA 98195
{xzhang,haralick,rameshv}@george.ee.washington.edu

Abstract

This paper describes a corner detection method that obtains maximum-aposteriori estimates for the corner location in a given sequence of points. We model an ideal corner as the intersection of two ideal line segments. The perturbations on the sample points in a given line segment are assumed to be i.i.d Gaussian random variables of zero mean and variance σ^2. Further, the perturbations on the points are assumed to be orthogonal to the ideal line. The paper discusses the theory of the corner detector and an algorithm that extends the basic theory to handle multilinear segment arcs. Experiments were conducted according to a specific protocol and performance curves showing the location error versus the noise variance, the included corner angle, and the arc length, are provided. Performance characterization of the corner detector is also performed by plotting the false alarm rate and the misdetect rate versus the context window length and included corner angle. It is shown that the experimental results match the theoretical error propagation.

1 Introduction

This paper describes a corner detector based on the maximum *a posteriori* (MAP) technique and Bayes theory to estimate corner locations on a given arc segment. The method can also be applied to polygonal linear approximation. We model an ideal corner as the intersection point of two straight lines. The corner detection model incorporates the prior distributions for corner model parameters. The detection procedure is extended to handle digital arc sequences with multiple corners by sliding a two-line-segment corner detector over the entire sequence iteratively to estimate corner positions and their related line parameters. The perturbations on the sample points in a given line segment are assumed to be i.i.d Gaussian random variables of zero mean and variance σ^2. Further, the perturbations on the points are assumed to be orthogonal to the ideal line. The paper discusses the theory of the corner detector, the theoretical analysis for the location error and experimental protocol used to evaluate the performance of the algorithm.

*Funding from ARPA is gratefully acknowledged.

2 Models and Algorithm

The ideal corner is the intersection point of two ideal line segments and in the continuous domain these two lines are specified by the equations: $rcos\theta_1 + csin\theta_1 - \rho_1 = 0$ and $rcos\theta_2 + csin\theta_2 - \rho_2 = 0$. The quantities in the expression $\theta_1, \theta_2, \rho_1, \rho_2$ can be derived from the coordinates of three points: (r_1, c_1), the starting point in line 1, (r_2, c_2), the intersection point of lines 1 and 2, and (r_3, c_3), the end point of line 2. The line segments are sampled to obtain a discrete sequence of points: $S =< \binom{r_i}{c_i} \mid i = 1, ..., I; (\hat{r}_i, \hat{c}_i) \in Z_R \times Z_C >$, where $Z_R \times Z_C$ is the image domain, and I is the number of points. An observed sequence of points $\hat{S}$ is assumed to be obtained by individually perturbing points (r_i, c_i) with i.i.d Gaussian samples with zero mean and standard deviation σ. Each point has a unique orientation specified by the orientation of the line segment in which the point belongs. The perturbations in the points are assumed to be introduced in the direction perpendicular to its orientation. Perturbations on the two line segments can be expressed by: $\hat{r}_i = r_i + \eta_i cos\theta_1$; $\hat{c}_i = c_i + \eta_i sin\theta_1$; $i = 1, ..., k$; $\hat{r}_i = r_i + \eta_i cos\theta_2$; $\hat{c}_i = c_i + \eta_i sin\theta_2$, ; $i = k+1, ..., I$, where $\eta_i \sim N(0, \sigma^2)$ and the ideal breakpoint is assumed to be at index k.

Prior Distributions – Assumptions

The parameters describing the ideal corner are $\theta_1, \theta_2, \rho_1, \rho_2, k$, and I. Certain assumptions on the nature of the prior distributions are made in this work. These assumptions are discussed here. The index k and parameters (θ_1, ρ_1) (θ_2, ρ_2) are independent of σ. Furthermore, the index k is independent of the line parameters (θ_1, ρ_1) (θ_2, ρ_2), and these line parameters are independent of the number of points I, therefore the prior probability distribution $P(k, \theta_1, \rho_1, \theta_2, \rho_2 \mid I)$ can be written as $P(\theta_2 \mid \theta_1)P(\rho_2)P(\rho_1 \mid \theta_1)P(\theta_1)P(k \mid I)$. We assume the index k to be uniformly dis-

tributed. That is:

$$P(k \mid I) = \begin{cases} K_k = 1/I - 2, & 2 \leq k \leq I-1, \\ 0, & \text{otherwise.} \end{cases}$$

Assume θ_1 to be uniformly distributed in the domain $[0, 2\pi)$, i.e. $P(\theta_1) = 1/2\pi$. We assume that the image domain is a square, ie. $Z = \mid Z_R \mid = \mid Z_C \mid$ and center at $(\mid Z_R \mid /2, \mid Z_C \mid /2)$. We also assume that ρ_1 is uniformly distributed in the interval $[0 \leq \rho_1 < Z)$. Thus: $P(\rho_1|\theta_1) = 1/Z$. Similarly, we assume that $P(\rho_2) = 1/Z, [0 \leq \rho_2 < Z)$. Let $\theta_{12} = \mid \theta_2 - \theta_1 \mid$ be defined in the domain of $[0, \pi]$. We assume the probability distribution of θ_{12} to be a truncated form of a Von Mises distribution with mean angle $\pi/2$. That is: $P(\theta_{12}) = K_1 e^{K_2 \sin(\theta_{12})}$. where K_1 is a scale factor and K_2 is a precision parameter for the angle.

Problem & Solution

Given a sequence of observations $\hat{S}$, the problem is to find the maximum aposteriori estimates for the index of the pixel corresponding to the corner location (k^*) and the line parameters $(\theta_1^*, \rho_1^*, \theta_2^*, \rho_2^*)$. That is: $(k^*, \theta_1^*, \rho_1^*, \theta_2^*, \rho_2^*) =$

$$\arg \max_{(k,\theta_1,\rho_1,\theta_2,\rho_2)} P(k, \theta_1, \rho_1, \theta_2, \rho_2 \mid \hat{S}, \sigma, I)$$

It can be shown that the logarithm of the aposteriori probability is given by $K - \frac{1}{2\sigma^2}\sum_{i=1}^{k}(\hat{r}_i cos\theta_1 + \hat{c}_i sin\theta_1 - \rho_1)^2 - \frac{1}{2\sigma^2}\sum_{i=k+1}^{I}(\hat{r}_i cos\theta_2 + \hat{c}_i sin\theta_2 - \rho_2)^2 + K_2 \sin(\mid \theta_2 - \theta_1 \mid)$, where $K = \log K_1 - \log(2\pi) - 2\log Z - \log(I-2) - I\log(\sqrt{2\pi}\sigma)$. Taking partial derivatives with respect to the parameters $\theta_1, \rho_1, \theta_2, \rho_2$ and setting the result to zero provides a system of non-linear equations. The initial solution to the non-linear equations is obtained by using maximum-likelihood estimation. A more precise solution is obtained by using gradient search. We do not provide the algorithm details here due to lack of space and more details can be found in [11].

In reality, we may be provided with pixel chains that contain more than one corner. We use the two-line-segment corner detector with a certain context window length and slide the window to perform detection on the entire arc. The procedure starts by examining the first I (assuming that I is the context window length) pixels of the given pixel chain. If a corner is detected, the corner detector moves to the next context window starting at the pixel next to the detected corner pixel. If the corner is not detected, the detector is moved along the sequence by a fixed step size (usually one pixel) and the detector is reapplied. We repeat this procedure until the tail of the context window reaches the end point of the given digital arc. The presence or absence of a corner within a given window is determined by a probability threshold. It can be easily shown that the value of the objective function is chisquare distributed (with I degrees of freedom) when there is no corner (i.e) $\theta_1 = \theta_2$. If T is the threshold on the value of the objective function, the probability of false alarm is given by: $Prob(X_1 < T_p) = \alpha_T$. Hence, we choose a confidence level α_T and set the threshold T_p so that $Prob(X_1 < T_p) = \alpha_T$. In reality, the objective function is evaluated at the estimates $\hat{\theta}_1$ and $\hat{\theta}_2$ and the minimum value is compared against T_p to determine if the breakpoint is significant or not.

3 Experimental Protocol and Results

In this section we describe the experimental protocol used to characterize the performance of the operator. Specifically, we measure: the precision of the estimated corner location as a function of the detector parameters, noise standard deviation and ideal corner model parameters, and the false alarm and misdetect characteristics. The input parameters to the corner detector are the context window length cwl, the estimated standard deviation of the noise σ, and the confidence coefficient α_{T_p}.

Two Line Segment Arc Generation

A perturbed two line segment arc, $\hat{S} = < (\hat{r}_i, \hat{c}_i); i = 1, ..., I >$, is generated in three steps. First, generate the coordinates of the points (r_i, c_i) on the digital line segments by discretizing the continuous line segments described with parameters $(r_1, c_1), L_1, \theta_1, \theta_{12}$, and L_2. Second, generate the sequence of samples $< m_i; i = 1, .., I >$, where each m_i; $i = 1, ..., I$ is an independent random sample coming from a Gaussian distributed random variable with zero mean and a standard deviation σ. Third, obtain a perturbed sequence of the arc segment by using the relations: $< (r_i + m_i \cos\theta_1, c_i + m_i \sin\theta_1); i = 1, \ldots, i^t >$, and $< (r_i + m_i \cos\theta_2, c_i + m_i \sin\theta_2); i = i^t + 1, \ldots, I >$.

Location Error Measurement

First, we measure the location errors versus noise standard deviation, the included corner angle and the arc sequence length. We apply the corner detector to synthetically generated two-line-segment sequences and obtain the distance between the true corner and the detected corner. For this experiment, the context window length is equal to the length of the sequence, σ is systematically set up, and α_{T_p} is not used. We let $\theta_{12} = 90°$, $L_1 = L_2 = 50$ units. For each $\sigma \in \{0.0, 0.2, 0.4, ..., 5.0\}$ and for all of $\theta_1 \in \{0°, 1°, ..., 359°\}$, we generate 10 sequences of

two-line-segment arcs. There are 360*10 runs, defined as N_{run}, for each σ. We apply the corner detector and obtain the root-mean-square error of the distance and the variance of this distance. Figures 1(a) and 1(b) are respectively the root-mean-square location error and the root-mean-square variance of the location error versus the noise standard deviation. It indicates that the error linearly increases as the noise increases and the variance of the error quadratically increases as the noise increases. It indicates that the theoretical computations and the experimental results are consistent.

We choose θ_{12} from the set $\{10°, 20°, ..., 170°\}$ and set $\sigma = 1.0$ to obtain plots shown in Figure 1(c), which illustrates the root-mean-square location error versus θ_{12}, and indicates that the detection has the tendency of having smaller error for 90° corner angle and larger error for corner angles away from 90°. In addition, the rather flat region around 90° corner angle indicates that the algorithm is more stable over a large range of corner angles. Figure 1(d) shows plots of the root-mean-square location error versus the arc length. The result indicates that the algorithm is stable with different arc lengths.

False alarm/Misdetect Characteristics

We evaluate the performance of the detector by plotting its false alarm rate and misdetection rate versus the context window length cwl, the included corner angle θ_{12} and the distance threshold d_0 which is a special parameter used during performance test. Here, cwl is chosen smaller than the sequence length, σ is systematically set up, and $\alpha_{T_P} = 0.9$. The false alarm rate is defined as the probability of noncorners being detected as corners, ie. $Prob$(detected as corners | $noncorners$), and the misdetection rate is defined as the probability of true corners not being detected as corners, ie. $Prob$(not detected as corners | true corners). Define a radius of d_0, called the distance threshold, centered at a true corner. If no point exists within the circle defined by the given radius, a misdetection happens. If the detected corner does not fall into any circular region of radius d_0 centered at a true corner, this detection is claimed as a false alarm.

We set $\theta_{12} = \pi/2$, $L_1 = L_2 = 50$ units, and $d_0 = 3$. For each context window length $cwl \in \{3, 4, \ldots, 70\}$, and $\theta_1 \in [0, 2*\pi)$ in increments of 1 degrees, we generate 10 sequeces of two line segment arcs. We apply the corner detector and plot the false alarm and misdetection rates. Figure 2(a) is the false alarm rate versus the context window length and it implies that the developed algorithm is more stable if a context window length is large enough to contain sufficient information for the estimation. Figure 2(b) is the misdetection rate versus the context window length and it shows that the rate drops linearly when the window length increases. Figure 2(c) and 2(d) show plots of the false alarm rate and the misdetection rates as a function of the included corner angle when $cwl = 2 * 50$ units. They show that the algorithm has small false alarm rate and misdetection rate around the 90°. Figure 3(a), 3(b) show the false alarm rate and the misdetection rate versus the distance threshold d_0 with $\theta_{12} = 90°$. These rates drops nonlinearly with the increase of the distance threshold d_0.

4 Conclusions

We have discussed a corner detector that is based on MAP estimation. We have evaluated the performance on synthetic data and have provided theoretical and empirical curves of performance. The experimental results showed that the theoretical and experimental results are consistent, and that this method is not very sensitive to random perturbations, is robust, stable and precise. More rigorous theoretical analysis of this operator is being done and future work will involve the theoretical and empirical comparison of our algorithm with traditional methods. We are also in the process of evaluating performance of our algorithm on a large collection of aerial images.

References

[1] Pavlidis, T., Algorithms for shape analysis of contours and waveforms", IEEE Trans. PAMI-2, pp.301-312, 1980.

[2] Dunham, J. G., "Optimum uniform piecewise linear approximation of planar curves", IEEE Trans. PAMI-8, pp.67-75, 1986.

[3] Ventura, J. A., and J.-M. Chen, "Segmentation of two-dimensional curve contours", *Pattern Recognition*, Vol 25. No.10, pp.1129-1140, 1992

[4] Rosenfeld, A., and E. Johnston, "Angle detection on digital curves", *IEEE Transactions on Computers*, 1973, pp. 875–878.

[5] Phillips, T.Y., and A. Rosenfeld, "An ISODATA algorithm for straight line fitting", *Pattern Recognition Letters*, Vol. 7, 1988, pp. 291–297.

[6] Zhang, X., and R. M. Haralick, "Bayesian corner detection", *Proc. of British Machine Vision Conference* BMVC'93, University of Surrey, Guildford. U.K. 21-23 September 1993.

[7] Leu, J.-G., and L. Chen, "Polygonal approximation of 2-D shapes through boundary merging", *Pattern Recognition Lett.*, 7 pp.231-238, 1988.

[8] Hemminger, T. L., and C. A. Pomalaza-Raez, "Polygonal representation: a maximum likelihood approach", *Comput. Vision Graphics Image Process*, 52 pp.239-247, 1990.

[9] F.J.Canny, "Finding edges and lines in images," Tech.Rep. 720, MIT AI Lab, June 1983.

[10] V. Ramesh, *et al*, "Automatic Tuning parameter seletection for feature extraction sequence," to appear in Proceedings of CVPR'94 conf. June 1994, Seattle, WA.

[11] X. Zhang et al, "Corner Detection using the MAP Technique," Intelligent Systems Lab Internal Report, University of Washington, Seattle, WA, 1994.

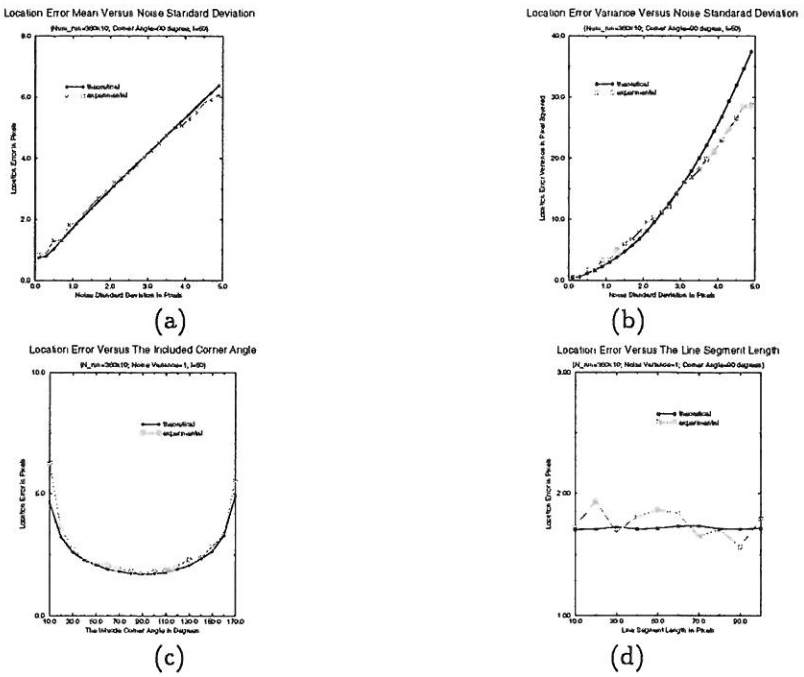

Figure 1: (a) Location error versus σ, (b) Variance of the location error versus σ, (c) Location error versus the included corner angle, and (d) Location error versus the arc length

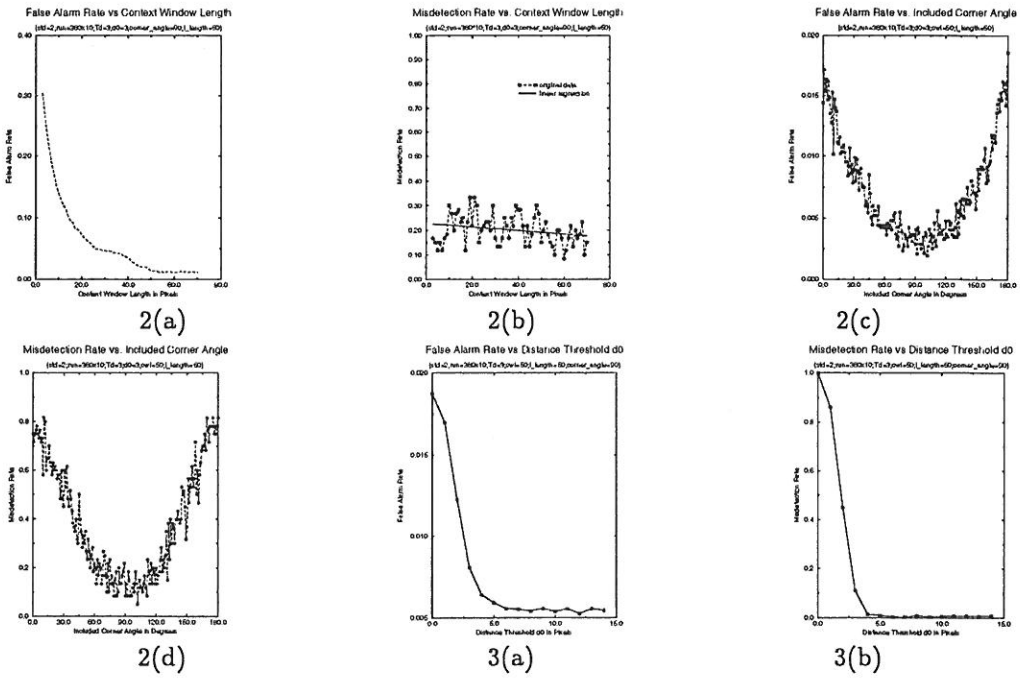

Figure 2: False alarm and Misdetection Characteristics. Figures 2 (a)-(d) and 3(a)-(b).

Corner Detection Using the MAP Technique

Xining Zhang, Robert M. Haralick, and Visvanathan Ramesh*

Intelligent Systems Laboratory
Department of Electrical Engineering, FT-10
University of Washington
Seattle, WA 98195
{xzhang,haralick,rameshv}@george.ee.washington.edu

Submitted to ICPR94

Send all correspondence to:
Xining Zhang
Department of Electrical Engineering, FT-10.
University of Washington
Seattle, Washington, 98195, USA

February 5, 1994

*Funding from ARPA is gratefully acknowledged.

Abstract

Corner detectors play an important role in arc segmentation, curve analysis, shape recognition, waveform segmentation and higher level image understanding. This paper develops a maximum a *posteriori* (MAP) based corner detection method which obtains the MAP estimates for the breakpoints (corners) along a given arc and the related parameters of the line between two successive corners. Our method utilizes a Bayesian framework and models an ideal corner as the intersection of two ideal line segments. The perturbations on the sample points, in a given line segment, are assumed to be i.i.d Gaussian random variables of zero mean and variance σ^2. Further, the perturbations on the points are assumed to be orthogonal to the ideal line. The paper discusses the theory of the corner detector, and an algorithm that extends the basic theory to handle multilinear segment arcs. The paper also discusses the theoretical analysis for the location error. Experiments were conducted according to a specific protocol and performance curves plotting location error versus the noise variance, the included corner angle, and the arc length, are provided. Performance characterization of the corner detector is also performed by plotting the false alarm rate and the misdetect rate versus the context window length and included corner angle. It is shown that the experimental results match the theoretical results. Results on real images are also presented.

1 Introduction

There are two primary groups of corner detection algorithms: one is based on detections directly from the underlying image[1–5], the other one is based on detections from arcs or curves[6–19] produced from previous low level image processing operations such as the edge detection or line finding followed by thinning, linking and labeling. In addition, some researchers[23] are also exploring corner detection based on the mixture of the above two methods. The corner detection approaches on arc segments can be used to detect dominant points for curve segmentation, so that shapes of object boundaries or meaningful curves can be described either by dominant points or parameters of the segmented curves between each pair of consecutive dominant points. Further, the shape can be analyzed and recognized[6–12].

This paper develops a corner detector based on the maximum a *posteriori* (MAP) technique and Bayes theory. The method uses a MAP-based corner detector to estimate corner locations on a given arc segment. The method is not only an arc segment corner detection scheme but also a way of polygonal linear approximation.

We model an ideal corner as the intersection point of two straight lines. The corner detection model incorporates the prior distributions for corner model parameters. If the prior information is ignored, the method becomes a maximum likelihood corner estimator or a maximum likelihood polygonal approximation of a planar curve. Therefore, our method is general and has wide applications.

The detection procedure is realized by sliding a two-line-segment corner detector over the entire sequence iteratively, in a precise manner, to estimate corner positions and their related lines. The corner detector model specifies a context window length as the detector length, which is the number of points for the obtained subsequence. Since the context window has a certain length and there will be only one corner to be estimated within the local region covered by the window, the estimation is locally optimized and more robust to random perturbations.

The paper first discusses the theory of the two-line-segment corner model and its detector in the Bayesian framework, and its application to multilinear segment arcs. Since the problem actually turns out as a nonlinear optimization problem, we also discuss a two step strategy for the optimization, The first step produces an initial estimate of the solution and the second step uses the gradient search to obtain the final approximation. Next, we describe the theoretical analysis for the location error of the detection. Finally we discuss the experiments and results for the proposed approach in synthetic data as well as real data.

2 Motivation and Theory

A corner happens on a discontinuity of the curvature of a curve and the location of the discontinuity can be approximated by two straight lines in its local neighborhood. In general, the discontinuity point is called the break point or the dominant point. If the curve is approximated by a polyline, dominant points are also called corners. Each corner has its own local neighborhood defined by the points on the two line segments forming the corner. Ideally when operations on a point seqeuence with multiple corners, we would like to detect only one corner in each neighborhood specified by two intersecting line segments. This idea motivates our MAP based corner detector.

2.1 Corner Model and Its Detector

We model an ideal corner by a two straight lines and their intersection. When given an observed sequence of ordered points, arising from two line segments, the detected corner is defined as the last observed point arising from the first estimated line segment. The following is the formalized problem statement:

<u>**Problem Statement**</u>

Given: an observed sequence of ordered points from an arc segment, $\hat{S} =< \binom{\hat{r}_i}{\hat{c}_i} \mid i = 1, ..., I; (\hat{r}_i, \hat{c}_i) \in Z_R \times Z_C >$, where $Z_R \times Z_C$ is the image domain, I is the number of points and $(\hat{r}_i, \hat{c}_i), i = 1, ..., I$ are the results of random perturbations on the points $(r_i, c_i), i = 1, ..., I$ constrained by two lines

$$\begin{aligned} r_i cos\theta_1 + c_i sin\theta_1 - \rho_1 &= 0, \quad i = 1, ..., k; \\ r_i cos\theta_2 + c_i sin\theta_2 - \rho_2 &= 0, \quad i = k+1, ..., I, \end{aligned}$$

where $\theta_j, \rho_j; j = 1, 2$ are line orientation and location parameters for the two line segments. and k is the index of the true corner position (r_k, c_k). Assume perturbations to be independently introduced on each sample point with the Gaussian distributed noise in the direction perpendicular to the line segment. Perturbations on the two line segments can be expressed by

$$\begin{aligned} \hat{r}_i &= r_i + \eta_i cos\theta_1; \quad \hat{c}_i = c_i + \eta_i sin\theta_1; \quad i = 1, ..., k; \\ \hat{r}_i &= r_i + \eta_i cos\theta_2; \quad \hat{c}_i = c_i + \eta_i sin\theta_2, ; \quad i = k+1, ..., I. \end{aligned}$$

where $\eta_i \sim N(0, \sigma^2)$.

Find: the estimated corner $(\hat{r}_{k^*}, \hat{c}_{k^*}), 2 \leq k^* \leq I-1$, along the arc $\hat{S}$ and the estimates of two line parameters, (θ_1^*, ρ_1^*) and (θ_2^*, ρ_2^*) so that

$$(k^*, \theta_1^*, \rho_1^*, \theta_2^*, \rho_2^*) = \arg \max_{(k,\theta_1,\rho_1,\theta_2,\rho_2)} P(k, \theta_1, \rho_1, \theta_2, \rho_2 \mid \hat{S}, \sigma, I)$$

By using Bayes theory, the maximization on the posterior probability can be converted to the maximization on the likelihood with prior probability, ie.

$$(k^*, \theta_1^*, \rho_1^*, \theta_2^*, \rho_2^*) = \arg \max_{(k,\theta_1,\rho_1,\theta_2,\rho_2)} P(\hat{S} \mid k, \theta_1, \rho_1, \theta_2, \rho_2, \sigma, I) P(k, \theta_1, \rho_1, \theta_2, \rho_2 \mid \sigma, I). \quad (1)$$

The first distribution of the right side of the equation is the likelihood of the given the two-line-segment corner detector model, perturbation quantity and the number of sample points. The model indicates that the observation $\hat{S}$ can be separated into two sub arc segments $\hat{S}_1$ $\hat{S}_2$, where, $\hat{S}_1 =< \binom{\hat{r}_i}{\hat{c}_i} \mid i = 1, .., k >$ and $\hat{S}_2 =< \binom{\hat{r}_i}{\hat{c}_i} \mid i = k+1, ..., I >$. Since perturbations on the first line (θ_1, ρ_1) are independent from those on the second line (θ_2, ρ_2), the likelihood of the observed $\hat{S}$ given two lines (θ_1, ρ_1) (θ_2, ρ_2) can be decomposed as

$$P(\hat{S} \mid k, \theta_1, \rho_1, \theta_2, \rho_2, \sigma, I) = P(\hat{S}_1 \mid k, \theta_1, \rho_1, \sigma, I) P(\hat{S}_2 \mid k, \theta_2, \rho_2, \sigma, I).$$

The perturbation model assumes that the Gaussian distributed noise is independently added onto each point of each line segment in the direction perpendicular to the line segment, the conditional probability of observing the first sub arc segment given the true line parameters is given by

$$\begin{aligned} P(\hat{S}_1 \mid k, \theta_1, \rho_1, \sigma, I) &= P(\hat{S}_1 \mid k, \theta_1, \rho_1, \sigma) \\ &= P((\hat{r}_1, \hat{c}_1)', ..., (\hat{r}_k, \hat{c}_k)' \mid \theta_1, \rho_1, \sigma) \\ &= \prod_{i=1}^{k} P((\hat{r}_i, \hat{c}_i)' \mid \theta_1, \rho_1, \sigma) \\ &= (\frac{1}{\sqrt{2\pi}\sigma})^k \prod_{i=1}^{k} e^{-\frac{1}{2\sigma^2}(\hat{r}_i cos\theta_1 + \hat{c}_i sin\theta_1 - \rho_1)^2}. \end{aligned}$$

Similarly, the conditional probability of observing the second sub arc segment $\hat{S}_2$ can be computed by

$$P(\hat{S}_2 \mid k, \theta_2, \rho_2, \sigma, I) = (\frac{1}{\sqrt{2\pi}\sigma})^{I-k} \prod_{i=k+1}^{I} e^{-\frac{1}{2\sigma^2}(\hat{r}_i cos\theta_2 + \hat{c}_i sin\theta_2 - \rho_2)^2}.$$

The index k and parameters (θ_1, ρ_1) (θ_2, ρ_2) are independent of σ therefore

$$P(k, \theta_1, \rho_1, \theta_2, \rho_2 \mid \sigma, I) = P(k, \theta_1, \rho_1, \theta_2, \rho_2 \mid I).$$

Furthermore, the index k is independent from the line parameters (θ_1, ρ_1) (θ_2, ρ_2), and these line parameters are independent of the number of points I, therefore the prior probability distribution

can be decomposed into

$$\begin{aligned} P(k, \theta_1, \rho_1, \theta_2, \rho_2 \mid I) &= P(\theta_2, \rho_2, \theta_1, \rho_1 \mid I) P(k \mid I), \\ &= P(\theta_2, \rho_2, \theta_1, \rho_1) P(k \mid I), \\ &= P(\theta_2 \mid \rho_2, \theta_1, \rho_1) P(\rho_2 \mid \theta_1, \rho_1) P(\rho_1 \mid \theta_1) P(\theta_1) P(k \mid I) \\ &= P(\theta_2 \mid \theta_1) P(\rho_2) P(\rho_1 \mid \theta_1) P(\theta_1) P(k \mid I). \end{aligned}$$

Assume the index k to be uniformly distributed between the second point and the second to the last point, ie.

$$P(k \mid I) = \begin{cases} K_k = 1/I - 2, & 2 \leq k \leq I - 1, \\ 0, & \text{otherwise.} \end{cases}$$

Assume θ_1 to be uniformly distributed in the domain $[0, 2\pi]$, ie. $P(\theta_1) = 1/2\pi$.

The conditional probability distribution $P(\rho_1 \mid \theta_1)$ is a probability density of the footprint of a line ρ_1 given a line orientation θ_1.

We assume that the image domain is a squared, ie. $Z = \mid Z_R \mid = \mid Z_C \mid$ and center at $(\mid Z_R \mid /2, \mid Z_C \mid /2)$. We also assume that the footprint of the line falls in the region of $[0 \leq \rho_1 < Z)$ (region R_I) with probability one, and in the region of $[Z \leq \rho_1 \leq \sqrt{2}Z]$ (region R_{II}) with probability zero, and that the distance of the line to the origin has a uniform distribution in region R_I and has probability zero in region R_{II}. Under these assumptions, the probability distribution of the first line location ρ_1 once given its line orientation θ_1 can be proved to be a constant of $1/Z$, ie $P(\rho_1 \mid \theta_1) = 1/Z$.

Similarly, we assume that ρ_2 has uniform distribution in the region of $[0 \leq \rho_2 < Z]$ and has zero probability in the region of $[Z \leq \rho_2 \leq \sqrt{2}Z]$, then $P(\rho_2) = 1/Z$.

The conditional probability distribution $P(\theta_2 \mid \theta_1)$ can be characterized by a probability of the angle difference between the two lines, ie.

$$P(\theta_2 \mid \theta_1) = P(\mid \theta_2 - \theta_1 \mid).$$

Let $\theta_{12} = \mid \theta_2 - \theta_1 \mid$ be defined in the domain of $[0, \pi]$. θ_{12} is called the included corner angle with an assumption of a larger preference around the right angle. This assumption is consistent with some practical applications such as roof corner detection of buildings in aerial images[24–26]. We assume the probability distribution of θ_{12} to be

$$P(\theta_{12}) = K_1 e^{K_2 \sin(\theta_{12})},$$

where K_1 and K_2 are two constants. K_2 can be estimated from the empirical distribution of θ_{12} by $\hat{K}_2 = 1/\hat{\sigma}^2_{\theta_{12}}$, and K_1 can be estimated by

$$\hat{K}_1 = \frac{1}{\int_0^{\pi} e^{\hat{K}_2 \sin(\theta_{12})} d\theta_{12}},$$

where $\hat{\sigma}^2_{\theta_{12}}$ is the estimated variance of the empirical distribution of θ_{12}.

[0]Note that this distribution is nothing but a truncated form of the Vonmises distribution.

Taking the logarithmic operation on equation 1, the optimization turns out the maximization problem on

$$K - \frac{1}{2\sigma^2}\sum_{i=1}^{k}(\hat{r}_i cos\theta_1 + \hat{c}_i sin\theta_1 - \rho_1)^2 - \frac{1}{2\sigma^2}\sum_{i=k+1}^{I}(\hat{r}_i cos\theta_2 + \hat{c}_i sin\theta_2 - \rho_2)^2 + +K_2 \sin(\mid \theta_2 - \theta_1 \mid),$$

where

$$K = \log K_1 - \log(2\pi) - 2\log Z - \log(I-2) - I\log(\sqrt{2\pi}\sigma).$$

2.2 Optimization of Parameter Estimations

The derivations result in a nonlinear optimization problem. In order to find the solution efficiently, quickly and more precisely, we use a two step procedure to find the approximate estimate of the solution. In the first step, we use maximum likelihood estimation to quickly find a good initial estimate and in the second step, we make use of gradient search scheme to find the more precisely estimate.

2.2.1 Initial Parameter Estimation

To maximize the posterior probability for a fixed k is to minimize

$$f(\theta_1, \rho_1, \theta_2, \rho_2) = \sum_{i=1}^{k}(\hat{r}_i \cos\theta_1 + \hat{c}_i \sin\theta_1 - \rho_1)^2 + \sum_{i=k+1}^{I}(\hat{r}_i \cos\theta_2 + \hat{c}_i \sin\theta_2 - \rho_2)^2 + g_1(\theta_1, \theta_2) \quad (2)$$

where $g_1(\theta_1, \theta_2) = -2\sigma^2 K_2 \sin(\mid \theta_2 - \theta_1 \mid)$. Let the first derivative of $f()$ with respect to ρ_1 be zero

$$\frac{\partial f}{\partial \rho_1} = 2\sum_{i=1}^{k}(\hat{r}_i \cos\theta_1 + \hat{c}_i \sin\theta_1 - \rho_1)(-1) = 0,$$

and ρ_1 can be estimated by

$$\hat{\rho}_1 = \cos\theta_1 \bar{r}(\hat{S}_1) + \sin\theta_1 \bar{c}(\hat{S}_1), \quad (3)$$

where

$$\bar{r}(\hat{S}_1) = \frac{1}{k}\sum_{i=1}^{k} r_i; \qquad \bar{c}(\hat{S}_1) = \frac{1}{k}\sum_{i=1}^{k} c_i.$$

Similarly, ρ_2 can be estimated by

$$\hat{\rho}_2 = \cos\theta_2 \bar{r}(\hat{S}_2) + \sin\theta_2 \bar{c}(\hat{S}_2), \quad (4)$$

where

$$\bar{r}(\hat{S}_2) = \frac{1}{I-k}\sum_{i=k+1}^{I} r_i; \qquad \bar{c}(\hat{S}_2) = \frac{1}{I-k}\sum_{i=k+1}^{I} c_i.$$

Let

$$\alpha = \begin{cases} \theta_2 - \theta_1, & 0 < \theta_2 - \theta_1 \leq \pi, \\ -(\theta_2 - \theta_1), & -\pi \leq \theta_2 - \theta_1 \leq 0. \end{cases} \tag{5}$$

Therefore, the objective function can be rewritten into a function only containing two explicit parameters

$$f(\theta_1, \theta_2) = G(\theta_1, \theta_2) + \sigma^2 K_2 \sin(\alpha(\theta_1, \theta_2)),$$

where

$$G(\theta_1, \theta_2) = \sum_{i=1}^{k} (\hat{r}_i \cos\theta_1 + \hat{c}_i \sin\theta_1 - \hat{\rho}_1)^2 + \sum_{i=k+1}^{I} (\hat{r}_i \cos\theta_2 + \hat{c}_i \sin\theta_2 - \hat{\rho}_2)^2.$$

In order to decrease the domain of search for minimumizing the good objective function, we can make good initial parameter guesses by obtaining θ_1 and θ_2 from the optimization only based on the two likelihood terms $G(\theta_1, \theta_2)$. Let the first order derivative of $G()$ with respect to θ_1 be zero.

$$\frac{\partial f}{\partial \theta_1} = 2\sum_{i=1}^{k} (\hat{r}_i \cos\theta_1 + \hat{c}_i \sin\theta_1 - \rho_1)(-\hat{r}_i \sin\theta_1 + \hat{c}_i \cos\theta_1) = 0, \tag{6}$$

Substitute the estimated ρ_1 from equation 3 into equation 6 and then obtain the following equation

$$\frac{1}{2}\sin 2\theta_1 [-\sum_{i=1}^{k} (\hat{r}_i - \bar{r}(\hat{S}_1))^2 + \sum_{i=1}^{k} (\hat{c}_i - \bar{c}(\hat{S}_1))^2] + \cos 2\theta_1 [\sum_{i=1}^{k} (\hat{r}_i - \bar{r}(\hat{S}_1))(\hat{c}_i - \bar{c}(\hat{S}_1))] = 0.$$

From this equation, the initial θ_1 can be estimated by

$$\hat{\theta}_1^{(0)} = \frac{1}{2}\tan^{-1} \frac{2\hat{\mu}_{rc}(\hat{S}_1)}{\hat{\mu}_{rr}(\hat{S}_1) - \hat{\mu}_{cc}(\hat{S}_1)},$$

where

$$\begin{aligned} \hat{\mu}_{rr}(\hat{S}_1) &= \frac{1}{k-1}\sum_{i=1}^{k} (\hat{r}_i - (\bar{r}(\hat{S}_1)))^2, \\ \hat{\mu}_{cc}(\hat{S}_1) &= \frac{1}{k-1}\sum_{i=1}^{k} (\hat{c}_i - (\bar{c}(\hat{S}_1)))^2, \\ \hat{\mu}_{rc}(\hat{S}_1) &= \frac{1}{k-1}\sum_{i=1}^{k} (\hat{r}_i - \bar{r}(\hat{S}_1))(\hat{c}_i - \bar{c}(\hat{S}_1)). \end{aligned}$$

Similarly, the initial θ_2 can be estimated by the derivatives of G with respect to θ_2,

$$\hat{\theta}_2^{(0)} = \frac{1}{2}\tan^{-1} \frac{2\hat{\mu}_{rc}(\hat{S}_2)}{\hat{\mu}_{rr}(\hat{S}_2) - \hat{\mu}_{cc}(\hat{S}_2)},$$

where

$$\hat{\mu}_{rr}(\hat{S}_2) = \frac{1}{I-k-1}\sum_{i=k+1}^{I}(\hat{r}_i - (\bar{r}(\hat{S}_2)))^2,$$

$$\hat{\mu}_{cc}(\hat{S}_2) = \frac{1}{I-k-1}\sum_{i=k+1}^{I}(\hat{c}_i - (\bar{c}(\hat{S}_2)))^2,$$

$$\hat{\mu}_{rc}(\hat{S}_2) = \frac{1}{I-k-1}\sum_{i=k+1}^{I}(\hat{r}_i - \bar{r}(\hat{S}_2))(\hat{c}_i - \bar{c}(\hat{S}_2)).$$

Once the good initial guesses on $\hat{\theta}_1^{(0)}$ and $\hat{\theta}_2^{(0)}$ have been estimated, the location parameter $\hat{\rho}_1^{(0)}$ and $\hat{\rho}_2^{(0)}$ can be estimated by

$$\hat{\rho}_1^{(0)} = \cos\hat{\theta}_1^{(0)}\bar{r}(\hat{S}_1) + \sin\hat{\theta}_1^{(0)}\bar{c}(\hat{S}_1),$$
$$\hat{\rho}_2^{(0)} = \cos\hat{\theta}_2^{(0)}\bar{r}(\hat{S}_2) + \sin\hat{\theta}_2^{(0)}\bar{c}(\hat{S}_2).$$

2.2.2 Parameter Modifications by Gradient Search

Once the initial guesses on $\theta_1^{(0)}$, $\theta_2^{(0)}$, $\rho_1^{(0)}$ and $\rho_2^{(0)}$ have been found, then more precise approximations of these parameters can be iteratively obtained by the gradient search method. Let current estimate vector be $\hat{\theta}^{(k)} = (\hat{\theta}_1^{(k)}, \hat{\theta}_2^{(k)})'$. and

$$\nabla G(\hat{\theta}^{(k)}) = (\frac{\partial G}{\partial \theta_1}, \frac{\partial G}{\partial \theta_2})'$$

then, a new estimate vector of $\hat{\theta}^{(k+1)}$ can be approximated by

$$\hat{\theta}^{(k+1)} = \hat{\theta}^{(k)} - \lambda^{(k)} \nabla G(\hat{\theta}^{(k)}),$$

where $\lambda^{(k)}$ is a sufficiently small positive scalar and $\hat{\theta}^{(k+1)} = (\hat{\theta}_1^{(k+1)}, \hat{\theta}_2^{(k+1)})'$. Once the $\hat{\theta}^{(k+1)}$ has been updated, ρ_1 and ρ_2 can be updated by

$$\hat{\rho}_1^{(k+1)} = \cos\hat{\theta}_1^{(k+1)}\bar{r}(\hat{S}_1) + \sin\hat{\theta}_1^{(k+1)}\bar{c}(\hat{S}_1),$$
$$\hat{\rho}_2^{(k+1)} = \cos\hat{\theta}_2^{(k+1)}\bar{r}(\hat{S}_2) + \sin\hat{\theta}_2^{(k+1)}\bar{c}(\hat{S}_2).$$

In the real application, the iteration can be stopped by inspecting whether $\nabla G(\hat{\theta}^{(k)}) = 0$ or $| G(\hat{\theta}^{(k+1)}) - G(\hat{\theta}^{(k)}) | \leq \epsilon$, depending on which is first satisfied, where the ϵ is a small constant.

When $0 < \theta_2 - \theta_1 \leq \pi$, equation 6 can be rewritten as

$$f(\theta_1, \theta_2) = G(\theta_1, \theta_2) - 2\sigma^2 K_2 \sin(\theta_2 - \theta_1).$$

In terms of equation 6 and the computations for $\hat{\mu}_{rr}(\hat{S}_j), \hat{\mu}_{cc}(\hat{S}_j)$ and $\hat{\mu}_{rc}(\hat{S}_j); j = 1, 2$, then

$$\frac{\partial f}{\partial \theta_1} = A_1 \sin 2\theta_1 + B_1 \cos 2\theta_1 - 2\sigma^2 K_2 \cos(\theta_2 - \theta_1)(-1),$$
$$\frac{\partial f}{\partial \theta_2} = A_2 \sin 2\theta_2 + B_2 \cos 2\theta_2 - 2\sigma^2 K_2 \cos(\theta_2 - \theta_1),$$

where

$$\begin{aligned} A_1 &= (k-1)(\hat{\mu}_{cc}(\hat{S}_1) - \hat{\mu}_{rr}(\hat{S}_1)), \\ B_1 &= 2(k-1)\hat{\mu}_{rc}(\hat{S}_1), \\ A_2 &= (I-k-1)(\hat{\mu}_{cc}(\hat{S}_2) - \hat{\mu}_{rr}(\hat{S}_2)), \\ B_2 &= 2(I-k-1)\hat{\mu}_{rc}(\hat{S}_2), \end{aligned}$$

When $-\pi \leq \theta_2 - \theta_1 \leq 0$,

$$\begin{aligned} \frac{\partial f}{\partial \theta_1} &= A_1 \sin 2\theta_1 + B_1 \cos 2\theta_1 + 2\sigma^2 K_2 \cos(\theta_2 - \theta_1)(-1), \\ \frac{\partial G}{\partial \theta_2} &= A_2 \sin 2\theta_2 + B_2 \cos 2\theta_2 + 2\sigma^2 K_2 \cos(\theta_2 - \theta_1). \end{aligned}$$

2.3 Application to Multi Linear Segment Models

In general, arc segments may contain more than one corner. In this case, we can use the two-line-segment corner detector with a certain context window length and slide the window to perform detection on the entire arc. From the previous section, we know that a break point is determined in terms of the maximum posteriori probability and always found when the two line segment corner detector is put on a sub arc segment of the underlying arc within a context window. However, the breaking point is not always corresponding to a corner point in the sub arc segment covered by the context window. Sometimes, there is no true corner located in the sub arc segment. In this case, the breaking point has nothing to do with the true corner point and therefore the breaking point should not be claimed as a detected corner point. If there is a true corner related to the detected break point, the break point can be claimed as a detected corner point. Therefore, there should be a way of determining whether the detected break point can be claimed as a corner or not.

We first concentrate on the likelihood part of the detector. The maximization of the likelihood of the observation from the estimated corner model is equal to the minimization of

$$X_1 = \frac{1}{\sigma^2}\sum_{i=1}^{k}(\hat{r}_i \cos\theta_1 + \hat{c}_i \sin\theta_1 - \rho_1)^2 + \frac{1}{\sigma^2}\sum_{i=k+1}^{I}(\hat{r}_i \cos\theta_2 + \hat{c}_i \sin\theta_2 - \rho_2)^2 \tag{7}$$

In the situation where there is no corner $\theta_1 = \theta_2$ X_1 would be a χ^2 distributed random variable with I degrees of freedoms.

The probability of false alarm given a threshold T_p for the objective function minimum is given by

$$Prob(X_1 < T_p) = \alpha_T.$$

This is the probability that a $Chi_{s}quare$ random variable with I degrees of freedom is less thatn T_p.

Hence, we choose a confidense level α_T and se the threshold T_p so that $Prob(X_1 < T_p) = \alpha_T$. In reality, we have two estimates for the angles of the lines $\hat{\theta}_1$ and $\hat{\theta}_2$ and we compute the quantity:

$$X_2 = min\{\frac{1}{\sigma^2}\sum_{i=1}^{I}(\hat{r}_i \cos\hat{\theta}_1 + \hat{c}_i \sin\hat{\theta}_1 - \rho_1)^2, \frac{1}{\sigma^2}\sum_{i=1}^{I}(\hat{r}_i \cos\hat{\theta}_2 + \hat{c}_i \sin\hat{\theta}_2 - \rho_2)^2\}, \tag{8}$$

and then compare X_2 with the determined threshold T_p.

If X_2 is larger than T_p, the estimated break point is claimed as a detected corner. Otherwise, the estimated breaking point is not claimed as a corner.

The motivation of the criterion can be explained as follows: if there is no corner, ie. (θ_1, ρ_1) is same as (θ_2, ρ_2), X_1 is a χ^2 distributed random variable but X_2 is not a χ^2 distributed random variable, since the minimum of the two dependent χ^2 random variable is not χ^2 distributed. Intutively, X_2 is a statistic that computes the minimum error that could be obtained by using the left or the right line segment as the true line segment. The minimum error corresponds tothe line segment $(\hat{\theta}_i, \hat{\rho}_i)$ that is the best approximation to the entire sequence. From the intuition of checking X_2, whenever exists a estimated corner, ie. $\theta_1 \neq \theta_2$, there will be almost $X_2 > X_1$, and when the line orientation difference $\theta = \theta_2 - \theta_1$ increases, the X_2 has a tendency of having large population larger than T_p.

Once the comparison is implemented, the algorithm can determine whether the break point is a corner or not in the sub arc segment. If no corner is claimed, move the detector along the given arc by a defined step (usually, we utilize one unit step). Once a corner has been claimed, move the detector to the next sub segment while keeping the head (staring point) of the detector window on the just detected corner. Repeat this procedure until the tail (ending point) of the detector window reaches the ending point of the given arc. This procedure works like a filter window sliding along the arc on which corners need to be estimated.

3 Location Error

Define the squared location error by the location distance between the detected corner position and the true corner position, ie.

$$d^2 = (\hat{r}_{k^*} - r^\circ)^2 + (\hat{c}_{k^*} - c^\circ)^2, \tag{9}$$

where k^* is the index of the estimated corner position (r^*, c^*), (r°, c°) is the true corner position indexed by k°. From the perturbation model, when $2 \leq k^* \leq k^\circ$,

$$\hat{r}_{k^*} = r_{k^*} + \eta_{k^*} \cos\theta_1^\circ; \quad \hat{c}_{k^*} = c_{k^*} + \eta_{k^*} \sin\theta_1^\circ. \tag{10}$$

when $k^\circ < k^* \leq I - 2$,

$$\hat{r}_{k^*} = r_{k^*} + \eta_{k^*} \cos\theta_2^\circ; \quad \hat{c}_{k^*} = c_{k^*} + \eta_{k^*} \sin\theta_2^\circ. \tag{11}$$

where $\eta_k^* \sim N(0, \sigma^2)$.

It can be proved that

$$d^2 = (r_{k^*} - r^\circ)^2 + (c_{k^*} - c^\circ)^2 + \eta_{k^*}^2, \tag{12}$$

where $k^* \in [2, I-2]$,

Let $\Phi = (\hat{S}, \Theta, \sigma)'$, where $\Theta = (\theta_1^\circ, \rho_1^\circ, \theta_2^\circ, \rho_2^\circ)'$. The distance d^2 can be estimated using its mean by,

$$E[d^2 \mid \Phi] \;=\; E[(r_{k^*} - r^\circ)^2 \mid \Phi] + E[(c_{k^*} - c^\circ)^2 \mid \Phi] + \sigma^2,$$

The quantity $(r_{k^*} - r^\circ)^2 + (c_{k^*} - c^\circ)^2$ is independent of $\eta_{k^*}^2$. Therefore, the variance of the squared distance can be proved to be

$$V[d^2 \mid \Phi] \;=\; E\{[(r_{k^*} - r^\circ)^2 + (c_{k^*} - c^\circ)^2]^2 \mid \Phi\} - \{E[(r_{k^*} - r^\circ)^2 \mid \Phi] + E[(c_{k^*} - c^\circ)^2 \mid \Phi]\}^2 + 2\sigma^4,$$

where

$$\begin{aligned}
E[(r_{k^*} - r^\circ)^2 \mid \Phi] &= \sum_{i_1*=2}^{I-1} (r_{k^*} - r^\circ)^2 P(k^* \mid \Phi), \\
E[(c_{k^*} - c^\circ)^2 \mid \Phi] &= \sum_{i_1*=2}^{I-1} (c_{k^*} - c^\circ)^2 P(k^* \mid \Phi), \\
E\{[(r_{k^*} - r^\circ)^2 + (c_{k^*} - c^\circ)^2]^2 \mid \Phi\} &= \sum_{i_1*=2}^{I-1} [(r_{k^*} - r^\circ)^2 + (c_{k^*} - c^\circ)^2]^2 P(k^* \mid \Phi).
\end{aligned}$$

Since r_{k^*} c_{k^*} $k^* = 2, ..., I-1, r^\circ, c^\circ$ are known, then the location error can be computed if the conditional probability $P(k^* \mid \Phi)$ is solved. This probability can be considered as a function of an instance sequence of the random variable $\hat{S}$. Denote this function by

$$\mathcal{P}(\hat{S}(n)) = P(k^* \mid \hat{S}(n), \Theta, \sigma); \quad n = 1, ...N,$$

where N is the number of instances of $\hat{S}$. We can use the mean of $\mathcal{P}(\hat{S}(n))$ to estimate $P(k^* \mid \Phi)$ by

$$\hat{P}(k^* \mid \Phi) = \frac{1}{N} \sum_{n=1}^{N} \mathcal{P}(\hat{S}(n)) = \frac{1}{N} \sum_{n=1}^{N} P(k^* \mid \hat{S}(n), \Theta, \sigma),$$

where for each $\hat{S}(n)$,

$$P(k^* \mid \hat{S}(n), \Theta^\circ, \sigma), \;=\; \frac{P(\hat{S}(n) \mid k^*, \Theta, \sigma) P(k^* \mid \Theta, \sigma)}{\sum_{j=2}^{I-1} P(\hat{S}(n) \mid j, \Theta, \sigma) P(j \mid \Theta, \sigma)}$$

The conditional probability $P(\hat{S} \mid j, \Theta, \sigma)$ can be computed by

$$(\frac{1}{\sqrt{2\pi}\sigma})^I \prod_{i=1}^{j} e^{-\frac{1}{2\sigma^2}(\hat{r}_i \cos\theta_1^\circ + \hat{c}_i \sin\theta_1^\circ - \rho_1^\circ)^2} \prod_{j+1}^{I} e^{-\frac{1}{2\sigma^2}(\hat{r}_i \cos\theta_2^\circ + \hat{c}_i \sin\theta_2^\circ - \rho_2^\circ)^2}$$

$P(\hat{S}, \mid k^*, \Theta^\circ, \sigma)$ can be computed in the same way because $k^* \in \{j; j = 2, ..., I-1\}$. Since the estimated index k^* is independent of the true parameter Θ and the hyper constant of the

quantity σ, the probability $P(k^* \mid \Theta, \sigma)$ is just the probability $P(k^*)$. But we assumed that the prior distribution for the break point is a uniform distribution. This implies

$$P(k^*) = \begin{cases} \frac{1}{I-2} & 2 \leq k^* \leq I-1, \\ 0, & \text{otherwise} \end{cases}$$

Therefore, the conditional probability $P(k^* \mid \hat{S}(n), \Theta^\circ, \sigma)$ can be simply computed by

$$\frac{P(\hat{S}(n) \mid k^*, \Theta, \sigma)}{\sum_{j=2}^{I-1} P(\hat{S}(n) \mid j, \Theta, \sigma)}$$

4 Experimental Protocol and Results

This section contains three experiments: 1) the location error measurement, 2) the algorithm performance measurement, and 3) the application of the detector to real images. The first two experiments are implemented on the synthetically generated sequences. The third experiment is implemented on the data processed from real images.

The input parameters to the corner detector are the context window length cwl, the estimated standard deviation of the noise σ, and the confidence coefficient α_{T_P}.

The first two experiments utilize the synthetically generated two-line-segment sequences. Therefore, we first need to discuss the process of the two-line-segment sequence generation.

4.1 Two Line Segment Arc Generation

A two line segment arc can be generated in three steps:

1. Specify the starting point (r_1, c_1), the first line length L_1, the second line length L_2, the first line angle ϕ_1 and the included corner angle θ_{12}, where ϕ_1 is the counterclockwise angle between the first line and the row axis. In this step, for each line L_1 or L_2, if $\mid \cos\phi_j \mid \geq \mid \sin\phi_j \mid; j = 1, 2$, we sample the data by increasing the row coordinate by unit steps, otherwise, by increasing the column coordinate by unit steps. For the first ideal line generation, if $\mid \cos\phi_1 \mid \geq \mid \sin\phi_1 \mid$, then $S_1 =< (r_i, c_i) | r_i = r_1 + i;\ c_i = c_1 + i\tan(\phi_1) >; i = 0, ..., i^t$, where $i^t = \lfloor L_1 \cos\phi_1 \rfloor + 1$ otherwise, $S_1 =< (r_i, c_i) | r_i = r_1 + i\cot(\phi_1);\ c_i = c_1 + i >; i = 0, ..., i^t$, where $i^t = \lfloor L_1 \sin\phi_1 \rfloor$. For the second ideal line generation, if $\mid \cos\phi_2 \mid \geq \mid \sin\phi_2 \mid$, then, $S_2 =< (r_i, c_i) | r_i = L_1\cos\phi_1 + i - i^t; c_i = L_1 \sin\phi_1 + (i - i^t)\tan(\phi_2) >; i = i^t + 1, ..., I$, where $I = i^t + \lfloor L_2 \cos\phi_2 \rfloor$, otherwise, $S_2 =< (r_i, c_i) | r_i = L_1\cos\phi_1 + (i - i^t)\cot(\phi_2);\ c_i = L_1 \sin\phi_1 + i - i^t >, i = i^t + 1, ..., I$, where $I = i^t + \lfloor L_2 \sin\phi_2 \rfloor$. The true corner $(r^t, c^t) = (L_1\cos\phi_1, L_1\sin\phi_1)$.

2. Generate a sequence of samples $< m_i; i = 1, .., I >$, where each $m_i;\ i = 1, ..., I$ is an independent random sample coming from a Gaussian distributed random variable with zero mean and a standard deviation σ.

3. Obtain a perturbed sequence of the arc segment by $< (r_i + m_i\cos\theta_1, c_i + m_i\sin\theta_1); i = 1, \ldots, i^t >$, and $< (r_i + m_i\cos\theta_2, c_i + m_i\sin\theta_2); i = i^t + 1, \ldots, I >$.

Thus, a perturbed two line segment arc $\hat{S} =< (\hat{r}_i, \hat{c}_i); i = 1, ..., I >$ is generated.

4.2 Experiment One (Location Error Measurement)

In this experiment, we measure the location errors versus noise standard deviation, the included corner angle and the arc sequence length. When measuring the location error, we utilize synthetically generated two-line-segment sequences, and obtain the distance between the true corner and the detected corner. In this experiment, the context window length is equal to the length of the sequence, σ is systematically set up, and α_{T_P} is not used.

1. **Location error versus the noise standard deviation**

   - Let $\theta_{12} = 90°$, $L_1 = L_2 = 50$ units.
   - For each $\sigma \in \{0.0, 0.2, 0.4, ..., 5.0\}$ and for all of $\theta_1 \in \{0°, 1°, ..., 359°\}$, generate 10 sequences of two-line-segment arcs. There are 360*10 runs, defined as N_{run}, for each σ.
   - For each sequence, apply the corner detector, and obtain the squared location error by
   $$d_p^{2(n)} = (\hat{r}_{i_1}^{(n)} - r^{t(n)})^2 + (\hat{c}_{i_1}^{(n)} - c^{t(n)})^2,$$
   where $(\hat{r}_{i_1}^{(n)}, \hat{c}_{i_1}^{(n)}); n = 1, ..., N_{run}$ is the estimated corner and. $(r^{t(n)}, c^{t(n)}); n = 1, ..., N_{run}$ is the related true corner.
   - Obtain the root-mean-square error by
   $$\bar{d}_p = (\frac{1}{N_{run}} \sum_{n=1}^{N_{run}} d_p^{2(n)})^{\frac{1}{2}},$$
   and its related variance by
   $$var(d_p) = (\frac{1}{(N_{run} - 1)} \sum_{n=1}^{N_{run}} (d_p^{2(n)} - \bar{d}_p^2)^2)^{\frac{1}{2}}.$$

   The figure 1(a) and 1(b) are respectively the root-mean-square location error and the root-mean-square variance of the location error versus the noise standard deviation. It indicates that the error linearly increases as the noise increases and the variance of the error quadratically increases as the noise increases. It indicates that the theoretical computations and the experimental results are consistent.

2. **Location error versus the included corner angle**
   This experiment is the same as above except that θ_{12} is chosen from the set $\{10°, 20°, ..., 170°\}$ and $\sigma = 1.0$

   Figure 1(c) illustrates the root-mean-square location error versus θ_{12}, and indicates that the detection has the tendency of having smaller error for 90° included corner angle and larger error for included corner angles away 90°. In addition, the rather flat region around 90° corner angle indicates that the algorithm is more stable over a large range of corner angles.

3. **Location error versus the arc sequence length**
   This experiment is the same as that in the first case but at this time the arc length is varied from 10 to 100 by a step of 10 pixels and the two line segment lengths are kept the same, ie. $L_1 = L_2$.

   The figure 1(d) is the root-mean-square location error versus the arc length. The result indicates that the algorithm is stable with different arc lengths.

4.3 Experiment two (Performance Measurement)

Once the algorithm has been designed, it needs to be tested for its performance [22][27]. In this experiment, we test the performance of the detector by poltting its false alarm rate and misdetection rate versus the context window length *cwl*, the included corner angle θ_{12} and the distance threshold d_0 which is a special parameter used during performance test.

Here, *cwl* is chosen smaller than the sequence length, σ is systematically set up, and $\alpha_{T_P} = 0.9$.

The false alarm rate is defined as the probability of noncorners being detected as corners, ie.

$$Prob(\text{detected as corners} \mid noncorners)$$

and the misdetection rate is defined as the probability of true corners being not detected as corners, ie.

$$Prob(\text{not detected as corners} \mid \text{true corners}).$$

Define a radius of d_0, called the distance threshold, centered at a true corner. If no point exists within the given radius, a misdetection happens. If the detected corner does not fall into any region centered by a true corner with the given radius d_0, this detection is claimed as a false alarm. The smaller the rate, the better the detection.

Define

$$\begin{aligned}
f_{10} &= \#\{\text{misdetections}\} = \#\{\textit{true corners} \text{ not being detected as corners}\},\\
f_{11} &= \#\{\text{detections}\} = \#\{\textit{true corners} \text{ being detected as corners}\},\\
f_{01} &= \#\{\text{false alarm}\} = \#\{\textit{non-corners} \text{ being detected as corners}\},\\
f_{00} &= \#\{\text{non detections}\} = \#\{\textit{non-corners} \text{ not being detected as corners}\},
\end{aligned}$$

and define

$$\text{the false alarm rate} = \frac{f_{01}}{f_{01} + f_{00}}, \tag{13}$$

$$\text{the misdetection rate} = \frac{f_{10}}{f_{10} + f_{11}}, \tag{14}$$

1. **False alarm rate and misdetection rate versus the context window length.**

   Let $\theta_{12} = 90°$, $L_1 = L_2 = 50$ units, $T_d = 3$. For each $cwl \in \{3, 4, ..., 70\}$, where $cwl < 2 * 50$. and all of $\theta_1 \in \{0°, 1°, ..., 359°$, generate 10 sequences of two-line-segment arcs. For each context window length, there is $N_{run} = 360 * 10$ runs. For each generated curve, detect corners. Obtain the false alarm and misdetection rates.

   Figure 2(a) is the false alarm rate versus the context window length and it implies that the developed algorithm is more stable if a context window length is large enough to contain sufficient information for the estimation.

   Figure 2(b) is the misdetection rate versus the context window length and it shows that the rate drops linearly when the window length increases.

2. **False alarm rate and misdetection rate versus the included corner angle.** This experiment is the same as above except that the included corner angle θ_{12} at this time is varied from 1° to 179° by a step size of 1° and the context window length $cwl = 2 * 50$ unit.

   Figure 2(c) and (d) are the false alarm rate and the misdetection rate. They show that the algorithm has small false alarm rate and misdetection rate around the 90°.

3. **False alarm rate and misdetection rate versus the distance threshold d_0.** This experiment is the same above except that the distance threshold is varied from 0 to 15 pixels by a step size of 1 pixel and the included corner angle is fixed at 90°.

   Figure 3(a), (b) are the false alarm rate and the misdetection rate versus the distance threshold d_0. These rates drops nonlinearly with the increase of the distance threshold d_0.

4.4 Experiment Three (Real Image Application)

In this experiment, the corner detector operates on input produced by image processing operators which produce the desired pixel chains and applied to the real image.

The input to the corner detector is produced by using a modified version of the Canny Edge operator. The edge detector employed is a two step procedure. The first step involves the estimation of gradient magnitude (in the row and column directions). We use the slope facet operator, Haralick [28], for this step. The second step uses Canny's hysteresis linking procedure to perform edge linking. Canny [29], uses two thresholds:

- a high gradient threshold, T, to mark potential edge candidates and
- a low gradient threshold, T_2, that is used in order to include additional edge pixels.

The linking procedure is a boundary tracking procedure. First pixels with gradient magnitude greater than T are marked as candidate edge pixels. Then non-maxima suppression is performed by retaining only pixels whose gradients form local maxima. Starting from each potential edge candidate the procedure tracks the boundary by the examining each neighbor along the edgel (specified by the normal to the gradient direction) and including edge pixels if the gradient magnitude is greater than T_2. The tracking terminates when a candidate neighboring pixel having a gradient magnitude less than T_2 is encountered. The linking procedure produces ordered pixel chains. These chains are subsequently used as input to the corner extraction scheme. There is one parameter called *minimum chain length* Th_l to choose sequences during implementing the corner detection. If the sequence with its length less than Th_l, the sequence will not be implemented with the corner detector. In this way, we can avoid some small sequences which may be caused by perturbations or could be the sequences we are not interested. Figure 4 shows the corner detection result on real data. Figure 4.(a) is the extracted edges of the 3 cut model. Figure 4.(b) is the detected corners overlaid on the original image. Figure 4.(c) is the extracted edges of the building model. Figure 4.(d) is the detected corners overlaid on the original image where some small sequences are not applied with the corner detector.

5 Conclusions

We have discussed a corner detector that is based on MAP estimation. This detector has been developed based on a corner detector in terms of two straight line segments forming the included corner angle and the corner model can be iteratively applied to multilinear segment arcs. Not only can this method be used for digital arc corner detection, but the algorithm can also be applied to the curve polygonal approximation. In addition to the detection theory, we also provided a theoretical analysis for the errors in the estimates of location. The experimental results showed that the theoretical and experimental results are consistent, and that this method is less sensitive to random perturbations, more robust, stable and precise. In order to do the nonlinear optimization efficiently and more precisely, we utilized a two step search strategy: first finding good initial parameter guess and then using gradient search scheme to find more precise estimate of the parameters. More rigorous theoretical analysis of this operator has been done and future work will involve the theoretical and empirical comparison of our algorithm with traditional methods. We are also in the process of evaluating performance of our algorithm on a large collection of aerial images. Although we have some illustrations in out paper showing the results obtained for real data, we believe that a sound performance evaluation has to be done on a large collection of images. We are following the protocol described in [24], [25] to do this.

References

[1] Kitchen, L., and A. Rosenfeld, "Gray level corner detection", *Pattern Recognition Lett.*, **1**, pp.95-102, 1982.

[2] Zuniga, O. A., and R. M. Haralick, "Corner detection using the facet model", Proc. IEEE CVPR, pp.30-37, 1983.

[3] Guiducci, A., "Corner characterization by differential geometry techniques", *Pattern Reconition Lett.*, **8**, pp.311-318, 1988.

[4] Mehrotra, R., and S. Nichani, "Corner Detection", *Pattern Recognition*, Vol. 23, No. 11, pp.1223-1233, 1990.

[5] Deriche, R., and G. Giraudon, "Accurate corner detection: an analytical study", IEEE ICCV, 1990, pp.66-70.

[6] Pavlidis, T., "Waveform segmentation through functional approximation", *Transactions on Computers,* Vol. C-22, No. 7, 1973, pp. 689–697.

[7] —,"Algorithms for shape analysis of contours and waveforms", IEEE Trans. PAMI-2, pp.301-312, 1980.

[8] Dunham, J. G., "Optimum uniform piecewise linear approximation of planar curves", IEEE Trans. PAMI-8, pp.67-75, 1986.

[9] Ventura, J. A., and J.-M. Chen, "Segmentation of two-dimensional curve contours", *Pattern Recognition,* Vol 25. No.10, pp.1129-1140, 1992

[10] Davis, L.S., "Understanding shape: angles and sides", *IEEE Transactions on Computers,* Vol. C-26, No. 3, 1977, pp. 236–242.

[11] Freeman, H., "Shape description via the use of critical points", *Pattern Recognition,* Vol. 10, 1978, pp. 159–166.

[12] Shirai, Y., "A context sensitive line finder for recognition of polyhedra", *Artificial Intelligence,* Vol. 4, 1973, pp. 95–119.

[13] Rosenfeld, A., and E. Johnston, "Angle detection on digital curves", *IEEE Transactions on Computers,* 1973, pp. 875–878.

[14] Phillips, T.Y., and A. Rosenfeld, "An ISODATA algorithm for straight line fitting", *Pattern Recognition Letters,* Vol. 7, 1988, pp. 291–297.

[15] Haralick, R. M. and T. Y. Phillips, "Subpixel precision corner detection and localization,"

[16] Zhang, X., and R. M. Haralick, "Bayesian corner detection", *Proc. of British Machine Vision Conference* BMVC'93, University of Surrey, Guildford. U.K. 21-23 September 1993.

[17] Ramer, U., "An iterative procedure for the polygonal approximation of plane curves", *Computer Graphics and Image Processing,* Vol. 1, 1972, pp. 244–256.

[18] Leu, J.-G., and L. Chen, "Polygonal approximation of 2-D shapes through boundary merging", *Pattern Recognition Lett.*, **7** pp.231-238, 1988.

[19] Hemminger, T. L., and C. A. Pomalaza-Raez, "Polygonal representation: a maximum likelihood approach", *Comput. Vision Graphics Image Process*, **52** pp.239-247, 1990.

[20] Pei, S.-C., and C.-N., Lin, "The detection of dominant points on digital curves by scale-space filtering", Pattern Recognition Lett. Vol.25, No. 11, pp13-7-1314, 1992.

[21] Teh, C.-H., and R.T. Chin, "A scale-independent dominant point detection algorithm", in *Proceedings, IEEE Computer Society Conference on Computer Vision and Pattern Recognition,* Ann Arbor, Michigan, 1988, pp. 229–234.

[22] Haralick, R. M."Performance characterization in image analysis: Thinning, A Case in Point", Pattern Recognition Letters 13, 1992, pp. 5–12.

[23] Xie, X., R. Sudhakar, and H. Zhuang, "Corner detection by a cost minimization approach", *Pattern Recognition*, Vol. 26, No. 8. pp.1235-1243, 1993.

[24] Zhang, X., V. Ramesh and R. M. Haralick, "Groundtruth outline drawing protocol for buildings of the aerial imagery", ISL Tech. Report, Aug 1993.

[25] Zhang, X., R. M. Haralick, and *et al* "Experimental protocol for building roof corner detection in the aerial imagery", ISL, Tech. Report, 1993.

[26] Zhang, X., R. M. Haralick, and *et al* "Building roof corner detection in the aerial imagery", Document in prepapration, 1993.

[27] V. Ramesh and R.M.Haralick, "Performance characterization of Edge operators," Presented at the Special Session on Evaluation of Modern Edge Operators, Orlando SPIE Machine Vision and Robotics Conference, April 92.

[28] Haralick, R.M., *"Edge and region analysis for digital image data,"* Computer Graphics and Image Processing, Vol.12, 1980, pp. 60-73.

[29] F.J.Canny, "Finding edges and lines in images," Tech.Rep. 720, MIT AI Lab, June 1983.

[30] V. Ramesh, *et al*, "Automatic Tuning parameter seletection for feature extraction sequence," to appear in Proceedings of CVPR'94 conf. June 1994, Seattle, WA.

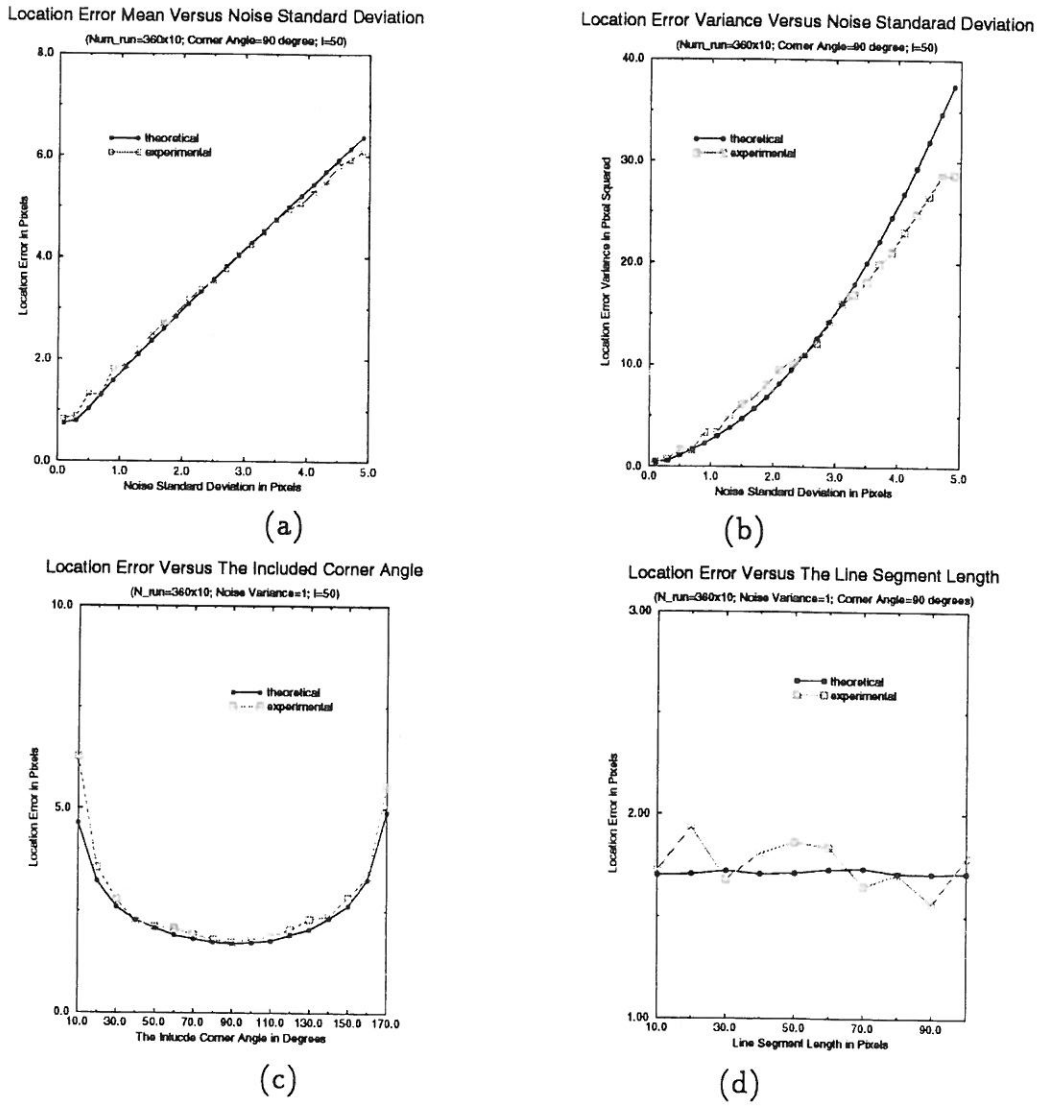

Figure 1: (a) Location error versus σ, (b) Variance of the location error versus σ, (c) Location error versus the included corner angle, and (d) Location error versus the arc length

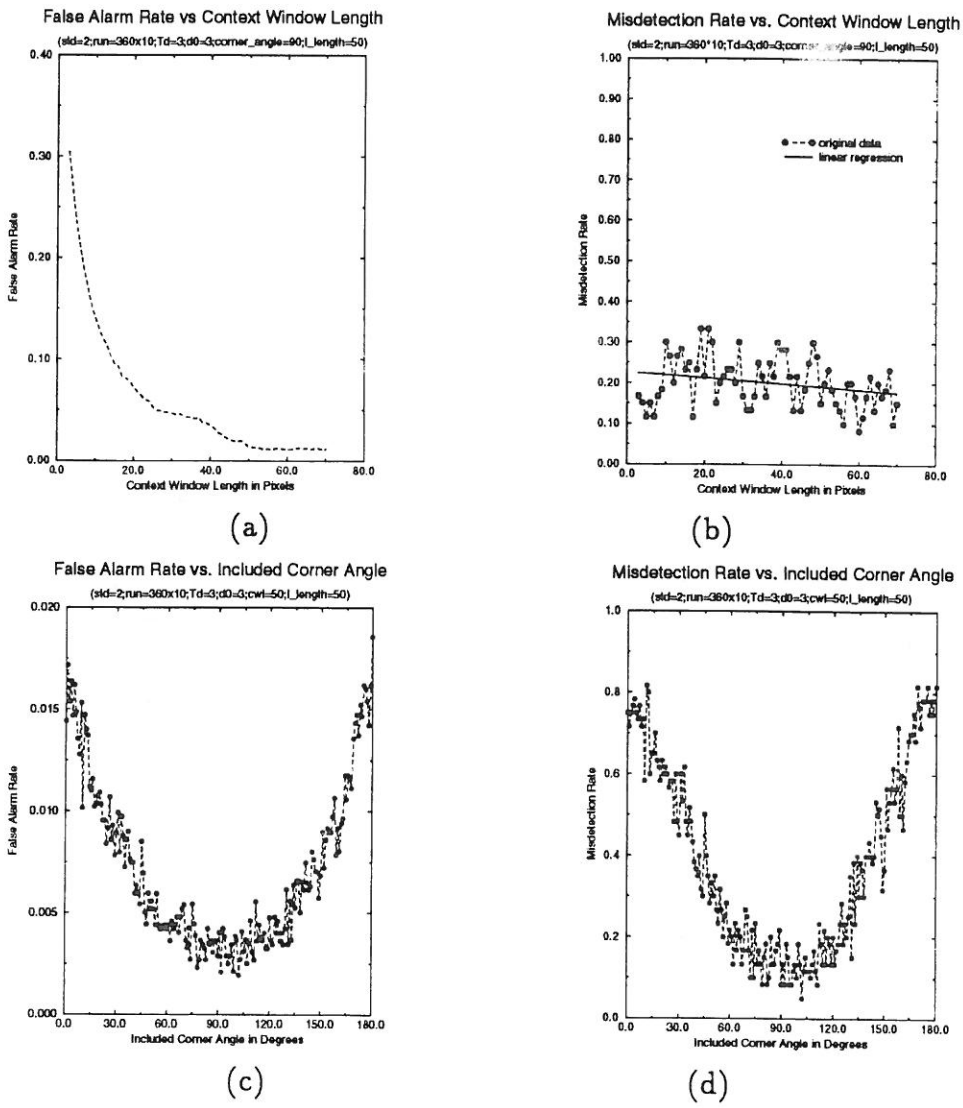

Figure 2: Performance operation measurement

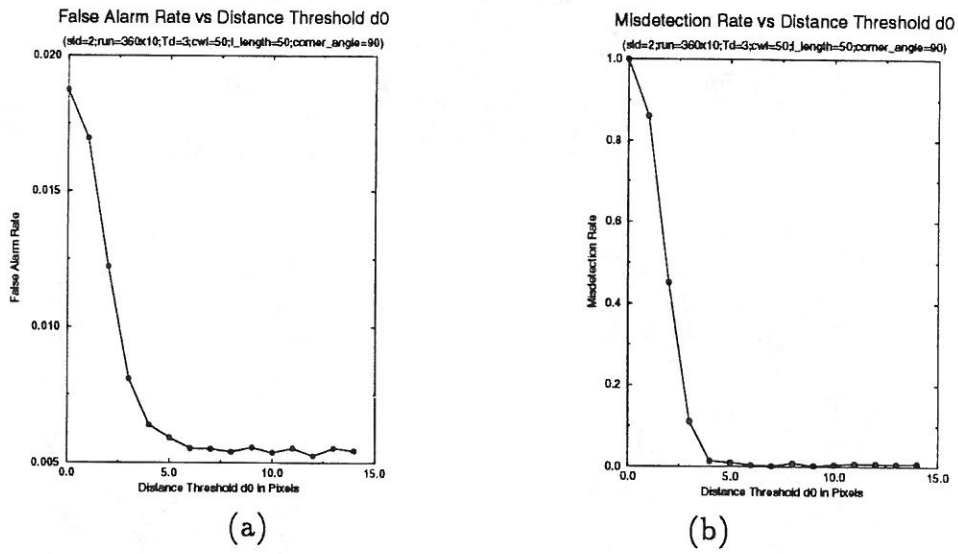

Figure 3: Performance operation measurement versus the distance threshold

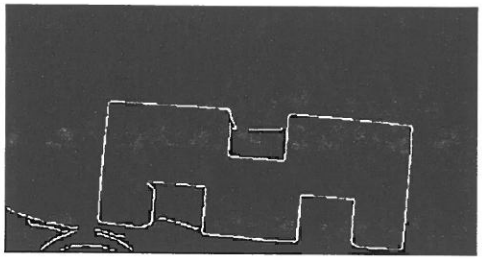

(a) edges

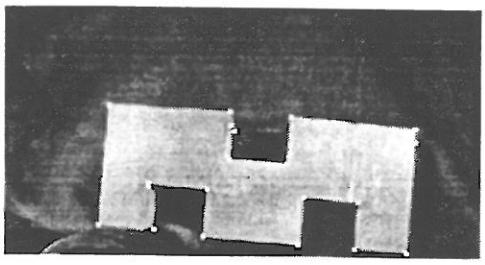

(b) corners

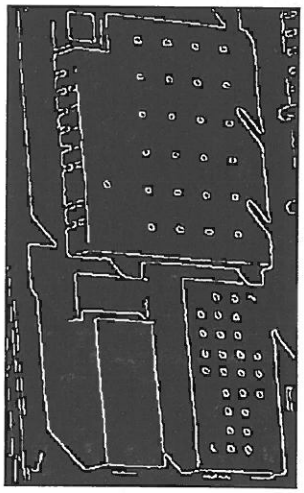

(c) edges

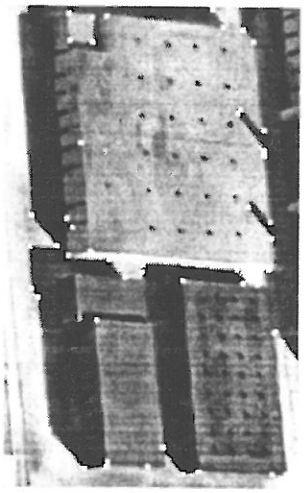

(d) corners

Figure 4: 4.(a) is the extracted edges of the 3 cut model. 4.(b) is the detected corners overlaid on the original image. 4.(c) is the extracted edges of the building model. 4.(d) is the detected corners overlaid on the original image